NIH Public Access
Author Manuscript
J Phys Chem B. Author manuscript; available in PMC 2014 August 08.

Published in final edited form as:
J Phys Chem B. 2013 August 8; 117(31): 9233–9240. doi:10.1021/jp4055186.

Epithelial-Mesenchymal Transition Enhances Nano-scale Actin Filament Dynamics of Ovarian Cancer Cells

Sunyoung Lee[#1], **Yang Yang**[#2], **David Fishman**[3], **Mark M. Banaszak Holl**[4], and **Seungpyo Hong**[2,*]

[1]Elmhurst Hospital Center, Icahn School of Medicine at Mount Sinai, Elmhurst, NY 11373

[2]Department of Biopharmaceutical Sciences, University of Illinois, Chicago, IL 60612

[3]Department of Obstetrics, Gynecology, and Reproductive Science, Icahn School of Medicine at Mount Sinai, New York, NY 10029

[4]Department of Chemistry, University of Michigan, Ann Arbor, MI 48109

[#] These authors contributed equally to this work.

Abstract

Epithelial ovarian cancer cells increase their capability of migration and invasion through the epithelial-mesenchymal transition (EMT), resulting in cell seeding and metastasis in the peritoneal cavity and onto adjacent organ surfaces. Cytoskeletal dynamics, such as those of the actin filament, have been speculated to play a role in enhanced cell motility; however, direct evidence has not been provided. Herein, we have directly measured pico- to nano-Newton-scale mechanical forces generated by actin dynamics of ovarian cancer SKOV-3 cells upon binding of integrin α5β1 to fibronectin (FN), i.e. formation of a focal adhesion, using real-time atomic force microscopy (AFM) in a force spectroscopy mode. The dendrimer surface chemistry through which FN was immobilized on the AFM probe surfaces further enhanced the sensitivity of the force measurement by 1.5 fold. Post-EMT SKOV-3 cells, induced by transforming growth factor (TGF-β), generated larger focal adhesion mechanical forces (17 nN and 41 nN before and after EMT, respectively) with faster migration than pre-EMT cells. Importantly, 22% of the forces transmitted through a single FN-integrin α5β1 pair from post-EMT cells were recorded to be sufficient to rupture the binding between FN and integrin α5β1 on the cells, which is not observed on pre-EMT cells. This implies that post-EMT cells, by generating forces strong enough to break the FN-integrin binding, migrate and metastasize beyond the ovary, whereas pre-EMT cancer cells are confined in the ovary without such force generation. These results demonstrate quantitative and direct evidence on the role of actin dynamics in the enhanced motility of post-EMT ovarian cancer cells, providing a fundamental insight into the mechanism of ovarian cancer metastasis.

Keywords

Epithelial ovarian cancer; metastasis; atomic force microscopy; focal adhesion; poly(amidoamine) dendrimer

[*]All correspondence should be addressed to: Prof. Seungpyo Hong, Ph.D., Department of Biopharmaceutical Sciences, College of Pharmacy, The University of Illinois at Chicago, 833 S. Wood St. Rm 335, Chicago, IL 60612, Phone: 312-413-8294, Fax: 312-996-0098, sphong@uic.edu.

Supporting Information **Available:** Schematic of AFM probe modification (Figure S1), AFM images of a fibronectin (FN)-immobilized probe (Figure S2), and RMS roughness and AFM imaging of probe surfaces (Figure S3) are included in the supporting information. This information is available free of charge via the Internet at http://pubs.acs.org.

NIH-PA Author Manuscript
NIH-PA Author Manuscript
NIH-PA Author Manuscript

NIH-PA Author Manuscript

NIH-PA Author Manuscript

NIH-PA Author Manuscript

I. Introduction

Ovarian cancer is the second most common gynecological malignancy and the leading cause of cancer death among women in the United States.[1, 2] The metastases from ovarian cancers, especially those with epithelial origin, are the primary reason for the high disease mortality.[3] Although not fully understood, self-seeding and metastases of cancer cells in the peritoneum cavity and adjacent organs are known to be the primary reason for high mortality of epithelial ovarian cancer.[4, 5] Epithelial ovarian cancer cells are particularly noteworthy as they are functionally flexible through the interconversion of epithelial and mesenchymal phenotypes via epithelial mesenchymal transition (EMT) or mesenchymal epithelial transition (MET).[1] After EMT, it has been reported that adhesion, migration, invasion, and metastasis of cancer cells are increased.[1, 6-8] The enhanced motility of those cells is reportedly initiated by the binding between integrin and extracellular matrix (ECM) molecules (specifically, integrin α5β1 and fibronectin (FN)), which induces an interaction of the actin cytoskeleton and intracellular molecules with focal adhesions.[1, 6, 9-13] As a result, focal adhesions generate actin cytoskeleton-mediated mechanical forces that enable cancer cells to migrate and adhere to underlying substrates.[14,15] However, the role of this mechanical force is poorly understood, particularly in the context of cancer cell migration, invasion, and metastasis.

In this study, we hypothesized that upon EMT, the actin-generated force towards the focal adhesion would become strong enough to dissociate the binding between a cell and ECM, making the ovarian cancer cell more motile and potentially invasive. To test the hypothesis, we conducted both direct, real-time force measurements and cell-level assays. By employing atomic force microscopy (AFM) with FN-immobilized probes, we directly measured pico- to nano-Newton (pN-nN)-scale forces generated by actin filament dynamics of human ovarian carcinoma SKOV3 cells upon binding to FN (i.e., focal adhesion formation). Generation 7 (G7) poly(amidoamine) (PAMAM) dendrimers were also used to improve the conjugation efficiency of FN molecules onto the AFM probe surfaces and to exploit the strong multivalent binding,[16] facilitating the association of actin filaments to focal adhesions. The force measurement revealed that post-EMT SKOV3 cells, unlike pre-EMT cells, generated forces sufficient to rupture the integrin-FN binding. Furthermore, wound-healing/cell migration experiments revealed that post-EMT SKOV-3 cells exhibited significantly enhanced motility compared to pre-EMT cells. The enhanced force generation and motility were blocked by treatment with cytochalasin D (CD), an inhibitor of actin polymerization and depolymerization, confirming that actin cytoskeleton dynamics were responsible for both observations. Here we report that actin-generated mechanical forces at the focal adhesions play a critical role in enhanced motility of ovarian cancer cells after EMT, which provides an insight into the mechanisms of ovarian cancer metastases.

II. Experimental Section

Materials

Spherical silicon AFM probe cantilevers (diameter: 5 μm, resonance frequency: 15 kHz) were purchased from Applied NanoStructures, Inc. (Santa Clara, CA, USA). Human epithelial ovarian SKOV-3 cells were obtained from American Type Culture Collection (ATCC, Manassas, VA, USA). Cell culture media - Gibco RPMI-1640, L-glutamine, antibiotics, and fetal bovine serum (FBS) were all purchased from Invitrogen™ (Grand Island, NY, USA). TGF-β and fibronectin were obtained from R&D Systems (Minneapolis, MN, USA). Phalloidin-tetramethyl rhodamine isothiocyanate (phalloidin-TRITC) was obtained from Molecular Probes, Inc. (Eugene, OR, USA). Sulfosuccinimidyl-4-(N-maleimidomethyl) cyclohexane-1-carboxylate (Sulfo-SMCC) was obtained from Pierce Biotechnology Inc. (Rockford, IL, USA). G7 PAMAM dendrimers, Cytochalacin D (CD),

NIH-PA Author Manuscript

NIH-PA Author Manuscript

NIH-PA Author Manuscript

Triton™ X-100, albumin (from bovine serum, BSA), 3-mercaptopropyl trimethoxysilane, *N*-(3-dimethylaminopropyl)-*N*′-ethylcarbodiimide hydrochloride (EDC), *N*-hydroxysuccinimide (NHS), and anhydrous ethanol were all purchased from Sigma (St. Louis, MO, USA). All other chemicals were also purchased from Sigma-Aldrich unless otherwise noted.

Functionalization of AFM cantilevers

Spherical silicon probe cantilevers were washed in absolute ethanol and treated with 3-mercaptopropyl trimethoxysilane (4% v/v in absolute ethanol) for 1 h under N_2, followed by gentle rinsing with ethanol for 10 min. The cantilevers were further incubated in ddH_2O containing sulfo-SMCC (2 mM) for 1.5 h. For some cantilevers, sulfo-SMCC was used as a linker for conjugation with G7 PAMAM dendrimers overnight (0.5 mg/mL, 90% surface carboxylation according to our previous report[16, 17]), followed by incubation with EDC (100 μM) and NHS (100 μM) for 15 min to activate the surface carboxyl groups. Fibronectin (FN, 1 mg/mL) was then incubated with both cantilevers with and without dendrimers for 2 h. After rinsing all the cantilevers with phosphate buffered saline (PBS), they were ready for imaging. The schematic of AFM probe modification was presented in Figure S1 (Supporting Information).

AFM force measurement and probe surface imaging

The photodiode sensitivity [nm/V] and spring constant [nN/nm] of AFM cantilevers were measured before AFM spectroscopy and imaging, following published reports.[18, 19] The functionalized AFM probes prepared as described above were placed on the SKOV-3 cell surfaces via an optical microscopy-aided AFM (Agilent 5500, Agilent technologies, Tempe, AZ, USA). Before the real-time measurement of actin cytoskeleton dynamics, the feedback loop was turned off to prevent it from offsetting the vertical deflection of cantilevered probes. Signal deflection [V] recorded in real time was multiplied by the pre-measured photodiode sensitivity [nm/V] and spring constant [nN/nm], which was ultimately converted to real-time force dynamics [nN]. Each force measurement was made on the surface of multiple cells and at different spots on the surface of the same cell. Multiple delta F's were found from one trace as defined as the force displacement between a trough to a peak (see Figure 1), and all the delta F's were collected from at least ten different cells (at least three spots of each cell). All statistical analyses were conducted with one-way ANOVA at $p < 0.05$.

SKOV-3 cell morphology observations

Human epithelial ovarian cancer cells, SKOV-3, were maintained in Gibco RPMI-1640 with L-glutamine supplemented with 10% (v/v) FBS and 1% (v/v) penicillin/streptomycin in a humidified incubator at 37°C and 5% CO_2. When cells were >90% confluent, the monolayer was detached from the cell culture flask by trypsin/EDTA and counted using a hemacytometer. For the cell morphology study, SKOV-3 cells were seeded in 8-well chamber slides (Millicell EZ Slide, Millipore, Billerica, MA, USA) at a density of 5,000 cells/well and incubated in the media. The cells were allowed to attach and stabilize overnight and rinsed twice with PBS. Fresh basal RPMI-1640 without FBS was used to maintain the cells in the incubator for 24 h. SKOV-3 cells were treated with TGF-β at different concentrations (10 and 20 ng/mL in fresh basal media) in duplicates for 24 h, as EMT induced by TGF-beta was experimentally verified by others.[7]

The actin cytoskeleton of SKOV-3 cells was stained with phalloidin-TRITC according to literature.[1] Briefly, the cells were washed twice with PBS, followed by fixation using a 3.7% formaldehyde solution in PBS for 10 min at room temperature. After being washed twice with PBS, cells were permeabilized using 0.1% Triton™ X-100 in PBS for 5 min. To reduce

NIH-PA Author Manuscript

NIH-PA Author Manuscript

NIH-PA Author Manuscript

non-specific background staining, cells were washed twice with PBS and incubated in 1% BSA in PBS for 30 min at room temperature. Phalloidin-TRITC (5 units/mL in PBS) was applied to each well and incubated for 30 min at room temperature. Cells were then washed twice with PBS and air-dried. The slides were treated with antiphotobleaching mounting media with DAPI (Vector Laboratory Inc., Burlingame, CA, USA) and covered with glass coverslips.

The stained actin cytoskeleton of SKOV-3 cells was visualized using an inverted microscope equipped with a fluorescence illuminator (IX 70-S1F2, Olympus America, Inc., Center Valley, PA, USA).[16] Images were recorded using a 40× objective and a CCD camera (QImaging Retiga 1300B, Olympus America, Inc., USA). SKOV-3 cell populations were also visualized using a Zeiss LSM 510 confocal laser scanning microscope (CLSM, Carl Zeiss, Germany).[20] The 543 nm line of a 1 mW tunable argon laser was used for excitation of TRITC, and a 25 mW diode UV 405 nm laser was used for excitation of DAPI. Emission was filtered at 565–595 and 420 nm for TRITC and DAPI, respectively. The aspect ratios of the phalloidin-TRITC stained cells were calculated using ImageJ software (NIH).[21] At least 200 cells were measured in each treatment group. The fluorescence intensities from the cells were measured using ImageJ (NIH) by comparing the relative brightness of pixels.

Cell migration assay

Cell migration assay was performed, following previous reports with adjustments.[22, 23] Briefly, a confluent monolayer of SKOV-3 cells in 24-well plates was incubated with or without 2 μg/mL of CD[24] in basal medium for 1 h in a humidified incubator at 37 °C and 5% CO_2. After removing CD and rinsing with pre-warmed PBS, cells were scratched with a 1 ml pipette tip and incubated in basal medium containing 20 ng/mL of TGF-β for 24 h. Cells were visualized under the inverted microscope at 0, 24, and 48 h. Images were recorded using a 4× objective and a CCD camera, and results were quantified by ImageJ software.

III. Results

To measure mechanical forces generated from cells in real time, we set up a system as illustrated in Figure 1a. The specific binding of FN and integrin α5β1[25, 26] through the FN-immobilized AFM probe placed on the apical surface of an SKOV-3 cell induced the formation of a focal adhesion between the cell surface and the probe contact area, as described elsewhere.[27, 28] The formation of focal adhesions on both apical and basal cell surfaces was previously verified by others using the optical tweezers and the magnetic bead twisting rheometry.[28, 29] Once FN was recognized by integrin α5β1, the actin cytoskeleton is known to physically connect to the FN-integrin α5β1 pairs and generate mechanical forces to the focal adhesion.[9] The mechanical forces generated as a result of actin-myosin interactions and dynamic actin polymerization/depolymerization[30-32] at the focal adhesion deflected the cantilevered probe, and the position of a laser beam reflected on the cantilever surface changed in situ on the photodetector surface. This was recorded as an electrical signal in the unit of volts [V] and converted to nN-scale force using the photodiode sensitivity [nm/V] and spring constant [nN/nm] of AFM cantilevers (Figure 1b).

The force measurement was performed using AFM force spectroscopy at close-to-microsecond resolution. Although many platform technologies have been reported for characterization of focal adhesion-generated forces,[14, 15,27, 28, 33] it is rare to provide tens of μ-second-scale, direct measurement of intracellular force evolution at focal adhesions. In this experiment, FN-immobilized spherical probes were placed on the surface of pre- and post-EMT SKOV-3 cells. As shown in Figure 2, nine different sets of force measurements were performed to monitor the force generation from focal adhesions: **1** G7 dendrimer-FN

NIH-PA Author Manuscript

NIH-PA Author Manuscript

NIH-PA Author Manuscript

probes on bare glass substrates as a control experiment to measure background noise signals ($\Delta F = 2.6 \pm 1.6$ nN); **2** fetal bovine serum (FBS)-adsorbed probes on SKOV-3 cells before the TGF-β-induced EMT as a control to measure non-specific bindings ($\Delta F = 3.0 \pm 2.1$ nN); **3** succinimidyl-4-(N-maleimidomethyl) cyclohexane-1-carboxylate (SMCC)-FN probes on pre-EMT cells ($\Delta F = 9.7 \pm 2.4$ nN); **4** G7 dendrimer-FN probes on pre-EMT cells ($\Delta F = 17.0 \pm 3.2$ nN); **5** G7 dendrimer-FN probes on pre-EMT cells after incubation with 2 μM of CD ($\Delta F = 2.1 \pm 1.5$ nN); **6** fetal bovine serum (FBS)-adsorbed probes on post-EMT cells ($\Delta F = 2.8 \pm 1.5$ nN); **7** SMCC-FN probes on post-EMT cells ($\Delta F = 31.4 \pm 6.9$ nN); **8** G7 dendrimer-FN probes on post-EMT cells ($\Delta F = 41.3 \pm 16.7$ nN); and **9** G7 dendrimer-FN probes on post-EMT cells after 2 μM of CD (2.5 ± 1.7 nN). The differences in the AFM-measured XFs among **1**, **2**, **5**, **6**, and **9** were not statistically significant ($p > 0.05$). In general, post-EMT SKOV-3 cells (**7** and **8**) generated greater forces than pre-EMT cells (**3** and **4**) in a given area of focal adhesions. The magnitudes of the measured force (tens of nN) at focal adhesions were also in good agreement with previously published data.[14, 15, 28, 34] The forces generated from both pre- and post-EMT SKOV-3 cells after incubation with CD (2-3 nN; **5** and **9**) were similar to the level of background noise measured on the bare glass and non-specific signals from the FBS-adsorbed probes (**1**, **2**, and **6**). These results confirmed that the real-time force dynamics are mediated by actin cytoskeletal dynamics. It was also noted that the force measurement sensitivity of G7 dendrimer-FN probes was increased by 1.5-fold compared to that of the SMCC-FN probes without dendrimers (see Figure S1 in the Supporting Information for the surface modifications of the AFM cantilevers). The increased force measurement using G7 dendrimers matches well with our previously published papers where we reported that dendrimers mediate multiple binding pairs to occur simultaneously in a highly localized area, achieving strong multivalent binding effect (up to a million fold enhancement in binding constant).[16, 35]

Next, we calculated the force exerted and transmitted through a single FN-integrin α5β1 pair using an AFM single molecule mapping technique that enables the mapping of the molecular distribution of FN on the probe surfaces, as described earlier.[19, 27] The nm-scale FN molecules were mapped and visualized on the FN-conjugated probe surface, based on which the number of FN-integrin α5β1 pairs on the probe surface was calculated. The contact area between an FN-conjugated probe (5 μm in diameter), and the cell surface was estimated to be 2.5 μm^2.[19] The number of FN-integrin pairs was calculated to be 640 ± 46 pairs that participate in active binding events in the contact area (Figure S2, Supporting Information). By dividing the nN-scale force measured at focal adhesions (Figure 2) by the calculated number of FN-integrin α5β1 pairs within the probe-cell contact area, we calculated the force generated through an individual FN-integrin pair of the complex. Note that all forces transmitted by individual FN-integrin α5β1 pairs were assumed to be equal. The loading rate [pN/sec] of actin cytoskeleton-mediated force was also calculated from force displacement (ΔF_i) divided by time duration (τ_i) (Figure 1 and 2). The loading rates and cytoskeletal forces transmitted through a FN-integrin α5β1 pair are plotted in Figure 3. Blue squares and connecting lines represent rupture forces of a single FN-integrin α5β1 pair, based on the results published elsewhere.[36] The rupture force is defined as the force required to break the binding of molecular pairs (See Figure 1a: $\Delta F > 0$, which is the pulling force exerted by the actin cytoskeleton). At a given loading rate, a force larger than the rupture force is sufficient to break the binding.[37] All the forces generated by pre-EMT SKOV-3 cells were smaller than the rupture force (Figure 3), which means these forces were not sufficient to break the binding of a FN-integrin α5β1 pair. In contrast, 22% of the forces generated by post-EMT SKOV-3 cells were larger than the rupture force (Figure 3), indicating that these forces are strong enough to break the binding of FN-integrin α5β1 pairs.[37]

NIH-PA Author Manuscript

NIH-PA Author Manuscript

NIH-PA Author Manuscript

To support the AFM results, we performed cell-level experiments to investigate changes in morphology and motility of SKOV-3 cells upon EMT. First, the actin cytoskeleton of SKOV-3 cells was stained and observed using confocal and fluorescence microscopy before and after EMT as shown in Figure 4. SKOV-3 cells before EMT were clustered in spherical, compact phenotypes and with less prominent actin stress fibers (Figure 4a and d). In contrast, upon treatment with TGF-β, SKOV-3 cells demonstrated mesenchymal stem cell-characteristic elongated and dispersed phenotypes with prominent actin stress fibers (Figure 4b, c, e, and f), which is consistent with previous reports confirming the occurrence of EMT in a comparable condition.[7] In the migration experiment (Figure 4g), post-EMT SKOV-3 cells migrated at a significantly higher rate than pre-EMT SKOV-3 cells. In addition, both pre- and post-EMT cells lost the stem cell-like phenotypic morphology and migration capacity after incubation with CD, an inhibitor of actin polymerization. We also measured the fluorescence intensity of polymerized actin filaments stained with Phalloidin-TRITC using ImageJ. The post-EMT cells exhibited greater actin filament staining (polymerization) compared to the pre-EMT cells. On average, the relative fluorescence intensity from the pre-EMT cells was 3.8 ± 1.1 (calculated using Image J), whereas that from the post-EMT cells was ranged from 6.1 ± 3.0 to 6.8 ± 1.7. This is consistent with our data obtained from the measurement of cell aspect ratios (in Figure 4 caption), which clearly demonstrates the morphological changes of the cells after TGF-β treatments. These results confirm that the actin cytoskeleton plays a key role in enhanced migration and motility of ovarian cancer cells after EMT.

IV. Discussion

In the AFM experiments, the number of FN that can be immobilized on the spherical AFM probe surface dictated the number of FN-integrin α5β1 pairs in the focal adhesion. Furthermore, both pre- and post-EMT cancer cells lost the mechanical force generation after incubation with CD. These results suggest that the reason for post-EMT cells generating larger scale forces than pre-EMT cells is probably due to the increased interaction with a dynamic actin cytoskeleton that can engage with the FN-integrin pairs, rather than the greater number of FN-integrin complexes themselves formed in the focal adhesion (Figure 5a). The fact that actin stress fibers become prominent in post-EMT cancer cells (Figure 4) further supports that the actin cytoskeleton is directly related to the larger mechanical force generation from post-EMT cancer cells. Interestingly, 22% of the actin-mediated forces transmitted through a single FN-integrin α5β1 pair in post-EMT SKOV-3 cells were larger than the rupture force, and yet 78% of the forces were not sufficient to rupture the pair (Figure 3). This provides an important clue in cancer cell migration and metastases, that is, post-EMT SKOV-3 cells maintain and stabilize the contact with the basal membranes by generating smaller forces (78%), and yet simultaneously migrate, crawl, and advance via larger forces (22%) that break the FN-integrin α5β1 binding. This could be explained using the analogy of a cliff climber. A climber stabilizes the body posture by holding a stone or a handle on the cliff with force that is not sufficient to break the hand-stone/handle complex. If the climber is strong or heavy enough to exert a large amount of force, the hand-stone/handle complex will be broken and he/she will not maintain the hand-stone/handle contact. This can be one of the reasons why post-EMT cancer cells, by generating greater force (22%) with which to break the integrin-FN binding, are mobile and metastatic, while maintaining their adhesion to the basal membranes (78% of the forces). By way of contrast, all forces from pre-EMT SKOV-3 cells are not sufficient to rupture the FN-integrin α5β1 pair (Figure 3), preventing them from being motile. This implies that pre-EMT SKOV-3 cells stabilize and fortify the adhesion on the basal membranes and cluster with other cancer cells (Figure 4) with little to no invasion potential, which is similar to the climber maintaining his/her posture on the cliff with an adequate amount of force that is not sufficient to break the hand-stone/handle complex.

NIH-PA Author Manuscript

NIH-PA Author Manuscript

NIH-PA Author Manuscript

Another interesting finding from our study is the enhanced immobilization of FN on the AFM probes through G7 PAMAM dendrimers. The force measured in focal adhesions using G7-FN probes was 1.5-fold greater than that using the SMCC-FN probes as mentioned above. In addition to the multivalent binding effect mediated by dendrimers,[16, 35] the reason for this can be inferred from the smaller RMS roughness of the G7-conjugated surfaces than that of other probe surfaces as shown in AFM images (Figure S3, Supporting Information). This measurement of RMS roughness confirms that G7 PAMAM dendrimers increase the conjugation efficiency by rendering the probe surfaces to be more uniformly conjugated with FN molecules. Thus, it implies that a larger number of the FN-integrin pairs were created in a given area of the focal adhesion in the case of the dendrimer-coated probe surfaces, increasing the sensitivity of the force measurement (Figure 5b). As mentioned above, we have published that sensitivity of cancer cell capture was increased by up to 7-fold using G7 PAMAM dendrimer-coated surfaces, most likely due to the dendrimers that allow for highly localized multiple binding pairs to simultaneously occur.[16] Given that cancer cell capturing is also mediated by the ligand-receptor interaction, the enhanced force measurement with the dendrimer-coated probes by 1.5-fold in this study is likely due to the combined effect of the multivalent binding and enhanced conjugation efficiency.

V. Summary

Taken together, our AFM measurements summarized in Figure 2 and 3 indicate that ovarian cancer SKOV-3 cells exert strong mechanical forces after EMT, as a result of enhanced actin cytoskeletal dynamics. The role of the actin dynamics is confirmed by the *in vitro* assays shown in Figure 4 where enhanced motility of the cells upon EMT was prohibited by CD treatment. Our results provide the experimental support, both in the molecular and cell level, that the actin filament dynamics plays a key role in increased motility of ovarian cancer cells upon EMT, which provides an explanation of one of the mechanisms of ovarian cancer metastases. Furthermore, the EMT and MET are not limited to epithelial ovarian cancer but also are observed in breast, colon, and esophageal cancers.[6] Therefore, the real-time force measurement studied herein could provide an effective platform tool for investigation of other cancers, particularly to elucidate the role of actin cytoskeleton dynamics in enhancement of the motile phenotype and could also be a tool to help evaluate the therapeutic potential of newly developed chemotherapeutics.

Supplementary Material

Refer to Web version on PubMed Central for supplementary material.

Acknowledgments

This work was conducted in a facility constructed with support from grant C06RR15482 from the NCRR, NIH. Authors thank Drs. Tracy Bohn Hemmerdinger and George S. Hagopian at Icahn School of Medicine at Mount Sinai for clinical and insightful discussions and Ming Fang (University of Michigan) for technical assistance. Thanks are extended to Drs. Michael Cho, Joanna Burdette, and Maria Barbolina of University of Illinois at Chicago for generously providing cells, compounds, and materials.

References

1. Vergara D, Merlot B, Lucot J-P, Collinet P, Vinatier D, Fournier I, Salzet M. Epithelial-Mesenchymal Transition in Ovarian Cancer. Cancer Lett. 2010; 291:59–66. [PubMed: 19880243]
2. Siegel R, Ward E, Brawley O, Jemal A. The Impact of Eliminating Socioeconomic and Racial Disparities on Premature Cancer Deaths. CA-Cancer J. Clin. 2011; 61:212–236. [PubMed: 21685461]

NIH-PA Author Manuscript

NIH-PA Author Manuscript

NIH-PA Author Manuscript

3. Burger RA, Brady MF, Bookman MA, Fleming GF, Monk BJ, Huang H, Mannel RS, Homesley HD, Fowler J, Greer BE, et al. Incorporation of Bevacizumab in the Primary Treatment of Ovarian Cancer. New Engl. J. Med. 2011; 365:2473–2483. [PubMed: 22204724]
4. Lengyel E. Ovarian Cancer Development and Metastasis. Am. J. Pathol. 2010; 177:1053–1064. [PubMed: 20651229]
5. Wang Y, Sheng Q, Spillman MA, Behbakht K, Gu H. Gab2 Regulates the Migratory Behaviors and E-Cadherin Expression Via Activation of the Pi3k Pathway in Ovarian Cancer Cells. Oncogene. 2012; 31:2512–2520. [PubMed: 21996746]
6. Micalizzi DS, Farabaugh SM, Ford HL. Epithelial-Mesenchymal Transition in Cancer: Parallels between Normal Development and Tumor Progression. J. Mammary Gland Biol. 2010; 15:117–134.
7. Cao L, Shao M, Schilder J, Guise T, Mohammad KS, Matei D. Tissue Transglutaminase Links Tgf-B, Epithelial to Mesenchymal Transition and a Stem Cell Phenotype in Ovarian Cancer. Oncogene. 2012; 31:2521–2534. [PubMed: 21963846]
8. Naora H, Montell DJ. Ovarian Cancer Metastasis: Integrating Insights from Disparate Model Organisms. Nat. Rev. Cancer. 2005; 5:335–366.
9. Wiesner S, Lange A, Fässler R. Local Call: From Integrins to Actin Assembly. Trends Cell Biol. 2006; 16:327–329. [PubMed: 16769214]
10. Sood AK, Armaiz, Pena GN, Halder J, Nick AM, Stone RL, Hu W, Carroll AR, Spannuth WA, Deavers MT, Allen JK, et al. Adrenergic Modulation of Focal Adhesion Kinase Protects Human Ovarian Cancer Cells from Anoikis. J. Clin. Invest. 2010; 120:1515–1523. [PubMed: 20389021]
11. Arnold M, Cavalcanti-Adam EA, Glass R, Blummel J, Eck W, Kantlehner M, Kessler H, Spatz JP. Activation of Integrin Function by Nanopatterned Adhesive Interfaces. ChemPhysChem. 2004; 5:383–388. [PubMed: 15067875]
12. Badgwell DB, Lu Z, Le K, Gao F, Yang M, Suh GK, Bao J-J, Das P, Andreeff M, Chen W, et al. The Tumor-Suppressor Gene Arhi (Diras3) Suppresses Ovarian Cancer Cell Migration through Inhibition of the Stat3 and Fak/Rho Signaling Pathways. Oncogene. 2012; 31:68–79. [PubMed: 21643014]
13. Sood AK, Coffin JE, Schneider GB, Fletcher MS, DeYoung BR, Gruman LM, Gershenson DM, Schaller MD, Hendrix MJ. Biological Significance of Focal Adhesion Kinase in Ovarian Cancer: Role in Migration and Invasion. Am. J. Pathol. 2004; 165:1087–1095. [PubMed: 15466376]
14. Legant WR, Pathak A, Yang MT, Deshpande VS, McMeeking RM, Chen CS. Microfabricated Tissue Gauges to Measure and Manipulate Forces from 3d Microtissues. Proc. Natl. Acad. Sci. U.S.A. 2009; 106:10097–10102. [PubMed: 19541627]
15. Sniadecki NJ, Anguelouch A, Yang MT, Lamb CM, Liu Z, Kirschner SB, Liu Y, Reich DH, Chen CS. Magnetic Microposts as an Approach to Apply Forces to Living Cells. Proc. Natl. Acad. Sci. U.S.A. 2007; 104:14553–14558. [PubMed: 17804810]
16. Myung JH, Gajjar KA, Saric J, Eddington DT, Hong S. Dendrimer-Mediated Multivalent Binding for Enhanced Capture of Tumor Cells. Angew. Chem. Int. Ed. 2011; 50:11769–11772.
17. Hong S, Rattan R, Majoros IJ, Mullen DG, Peters JL, Shi X, Bielinska AU, Blanco L, Orr BG, Baker JR, et al. The Role of Ganglioside Gm1 in Cellular Internalization Mechanisms of Poly(Amidoamine) Dendrimers. Bioconjugate Chem. 2009; 20:1503–1513.
18. Lee S, Mandic J, Van Vliet KJ. Chemomechanical Mapping of Ligand-Receptor Binding Kinetics on Cells. Proc. Natl. Acad. Sci. U.S.A. 2007; 104:9609–9614. [PubMed: 17535923]
19. Walton EB, Lee S, Van Vliet KJ. Extending Bell's Model: How Force Transducer Stiffness Alters Measured Unbinding Forces and Kinetics of Molecular Complexes. Biophys. J. 2008; 94:2621–2630. [PubMed: 18178658]
20. Yang Y, Sunoqrot S, Stowell C, Ji J, Lee C-W, Kim JW, Khan SA, Hong S. Effect of Size, Surface Charge, and Hydrophobicity of Poly(Amidoamine) Dendrimers on Their Skin Penetration. Biomacromolecules. 2012; 13:2154–2162. [PubMed: 22621160]
21. Prager-Khoutorsky M, Lichtenstein A, Krishnan R, Rajendran K, Mayo A, Kam Z, Geiger B, Bershadsky AD. Fibroblast Polarization Is a Matrix-Rigidity-Dependent Process Controlled by Focal Adhesion Mechanosensing. Nat. Cell Biol. 2011; 13:1457–1465. [PubMed: 22081092]
22. Liang CC, Park AY, Guan JL. In Vitro Scratch Assay: A Convenient and Inexpensive Method for Analysis of Cell Migration in Vitro. Nat. Protoc. 2007; 2:329–333. [PubMed: 17406593]

NIH-PA Author Manuscript

NIH-PA Author Manuscript

NIH-PA Author Manuscript

23. Kandala PK, Srivastava SK. Diindolylmethane Suppresses Ovarian Cancer Growth and Potentiates the Effect of Cisplatin in Tumor Mouse Model by Targeting Signal Transducer and Activator of Transcription 3 (Stat3). BMC Med. 2012; 10:1–18. [PubMed: 22216957]
24. Schliwa M. Action of Cytochalasin D on Cytoskeletal Networks. J. Cell Biol. 1982; 92:79–91. [PubMed: 7199055]
25. Mitra AK, Sawada K, Tiwari P, Mui K, Gwin K, Lengyel E. Ligand-Independent Activation of C-Met by Fibronectin and A5β1-Integrin Regulates Ovarian Cancer Invasion and Metastasis. Oncogene. 2011; 30:1566–1576. [PubMed: 21119598]
26. Shroff K, Kokkoli E. Pegylated Liposomal Doxorubicin Targeted to A5β1-Expressing Mda-Mb-231 Breast Cancer Cells. Langmuir. 2012; 28:4729–4736. [PubMed: 22268611]
27. Lee, S. Ph.D. thesis - Massachusetts Institute of Technology. 2009. Chemomechanics at the Cell;Material Interface: Measurements and Implications of Forced Molecular Unbinding.
28. Galbraith CG, Yamada KM, Sheetz MP. The Relationship between Force and Focal Complex Development. J. Cell Biol. 2002; 159:695–705. [PubMed: 12446745]
29. Van Vliet KJ, Bao G, Suresh S. The Biomechanics Toolbox: Experimental Approaches for Living Cells and Biomolecules. Acta Mater. 2003; 51:5881–5905.
30. Even-Ram S, Doyle AD, Conti MA, Matsumoto K, Adelstein RS, Yamada KM. Myosin Iia Regulates Cell Motility and Actomyosin–Microtubule Crosstalk. Nat. Cell Biol. 2007; 9:299–309. [PubMed: 17310241]
31. Giannone G, Dubin, Thaler BJ, Rossier O, Cai Y, Chaga O, Jiang G, Beaver W, Dobereiner H-G, Freund Y, Borisy G, et al. Lamellipodial Actin Mechanically Links Myosin Activity with Adhesion-Site Formation. Cell. 2007; 128:561–675. [PubMed: 17289574]
32. Zamir E, Katz M, Posen Y, Erez N, Yamada KM, Katz BZ, Lin S, Lin DC, Bershadsky A, Kam Z, et al. Dynamics and Segregation of Cell–Matrix Adhesions in Cultured Fibroblasts. Nat. Cell Biol. 2000; 2:191–196. [PubMed: 10783236]
33. Galbraith CG, Sheetz MP. A Micromachined Device Provides a New Bend on Fibroblast Traction Forces. Proc. Natl. Acad. Sci. U.S.A. 1997; 94:9114–9118. [PubMed: 9256444]
34. Gov NS. Modeling the Size Distribution of Focal Adhesions. Biophys. J. 2006; 91:2844–2847. [PubMed: 16861281]
35. Hong S, Leroueil PR, Majoros I. n. J. Orr BG, Baker JR Jr, Banaszak Holl MM. The Binding Avidity of a Nanoparticle-Based Multivalent Targeted Drug Delivery Platform. Chem. Biol. 2007; 14:107–115. [PubMed: 17254956]
36. Li F, Redick SD, Erickson HP, Moy VT. Force Measurements of the A5b1 Integrin–Fibronectin Interaction. Biophys. J. 2003; 84:1252–1262. [PubMed: 12547805]
37. Bell GI. Models for the Specific Adhesion of Cells to Cells. Science. 1978; 200:618–627. [PubMed: 347575]

NIH-PA Author Manuscript

NIH-PA Author Manuscript

NIH-PA Author Manuscript

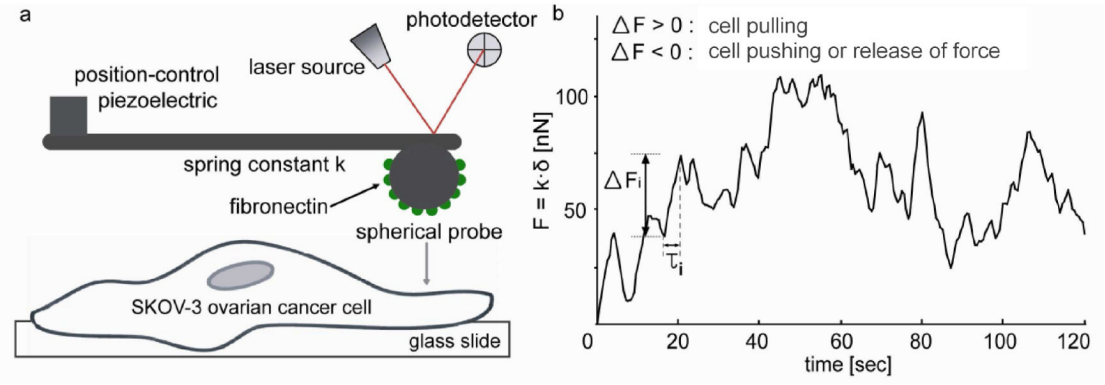

Figure 1.

Schematic of AFM measurement of force dynamics. (a) An FN-conjugated spherical probe (diameter = 5 μm) is localized on the SKOV-3 cell surface using an optical microscope-aided AFM. The physical contact of FN on the probe with the cell surface triggers the formation of a focal adhesion via the binding between FN and integrin α5β1 on the cell surface. This setup enables the real-time measurement of nano-scale forces generated through the physical connection of the actin cytoskeleton, integrin, and FN. (b) Deflection created by cellular force dynamics is recorded in real time using AFM force spectroscopy using the setup shown in (a) and analyzed in terms of force displacement (ΔF_i) and time duration (τ_i). ΔF_i is defined as the force displacement between a trough to a peak, and τ_i is time period during which ΔF_i is displaced as shown in (b).

NIH-PA Author Manuscript

NIH-PA Author Manuscript

NIH-PA Author Manuscript

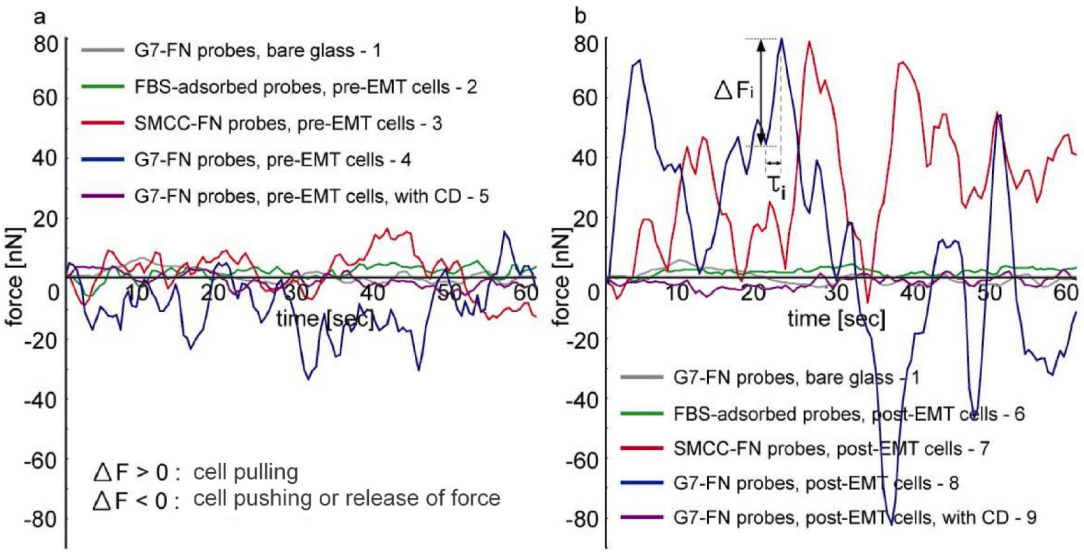

Figure 2.

Real-time force dynamics on SKOV-3 cell surfaces. (a) Cellular dynamics measured on SKOV-3 cells before TGF-β-induced EMT using the setup shown in Figure 1. (b) Cellular dynamics after TGF-β-induced EMT. Gray curves in (a) and (b) represent force signals with G7-FN probes on glass substrates; Green curves, with FBS-adsorbed probes on cells before and after EMT; Red curves, with SMCC-FN probes on cells before and after EMT; Blue curves, with G7-FN probes on cells before and after EMT; Purple curves, with G7-FN probes on cells after incubation with 2 μM of cytochalasin D before and after EMT.

NIH-PA Author Manuscript

NIH-PA Author Manuscript

NIH-PA Author Manuscript

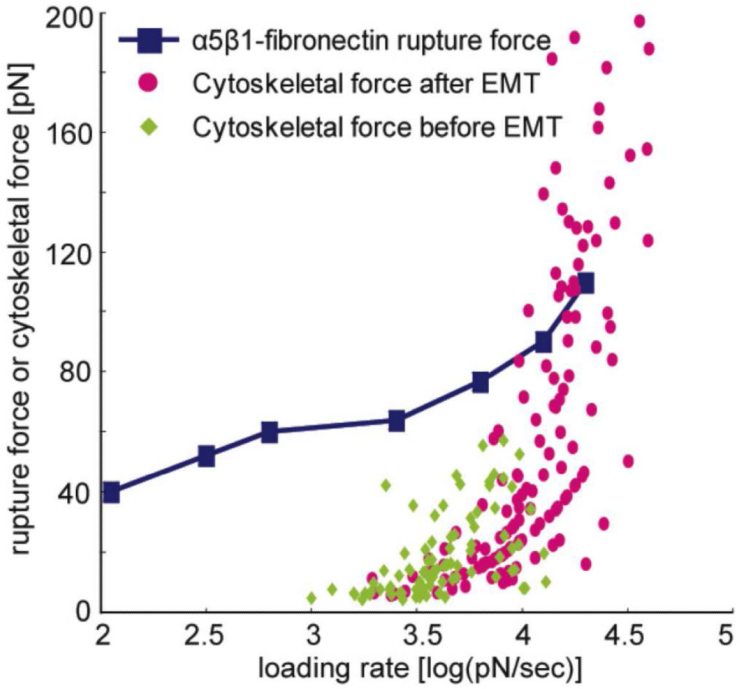

Figure 3.

Force transmitted through a single FN-integrin α5β1 pair and rupture force of FN-integrin α5β1 binding. Blue squares and connecting lines are rupture forces of a FN-integrin α5β1 pair at various loading rates (published data by Feiya Li 2003[36]); Green rhombi and pink circles represent cytoskeletal force transmitted through a single FN-integrin α5β1 pair measured using FN-conjugated probes before and after EMT, respectively. Note that 22% of cytoskeletal forces transmitted through a single FN-integrin α5β1 pair (pink circles) are larger than rupture forces (blue squares and connecting lines).

NIH-PA Author Manuscript
NIH-PA Author Manuscript
NIH-PA Author Manuscript

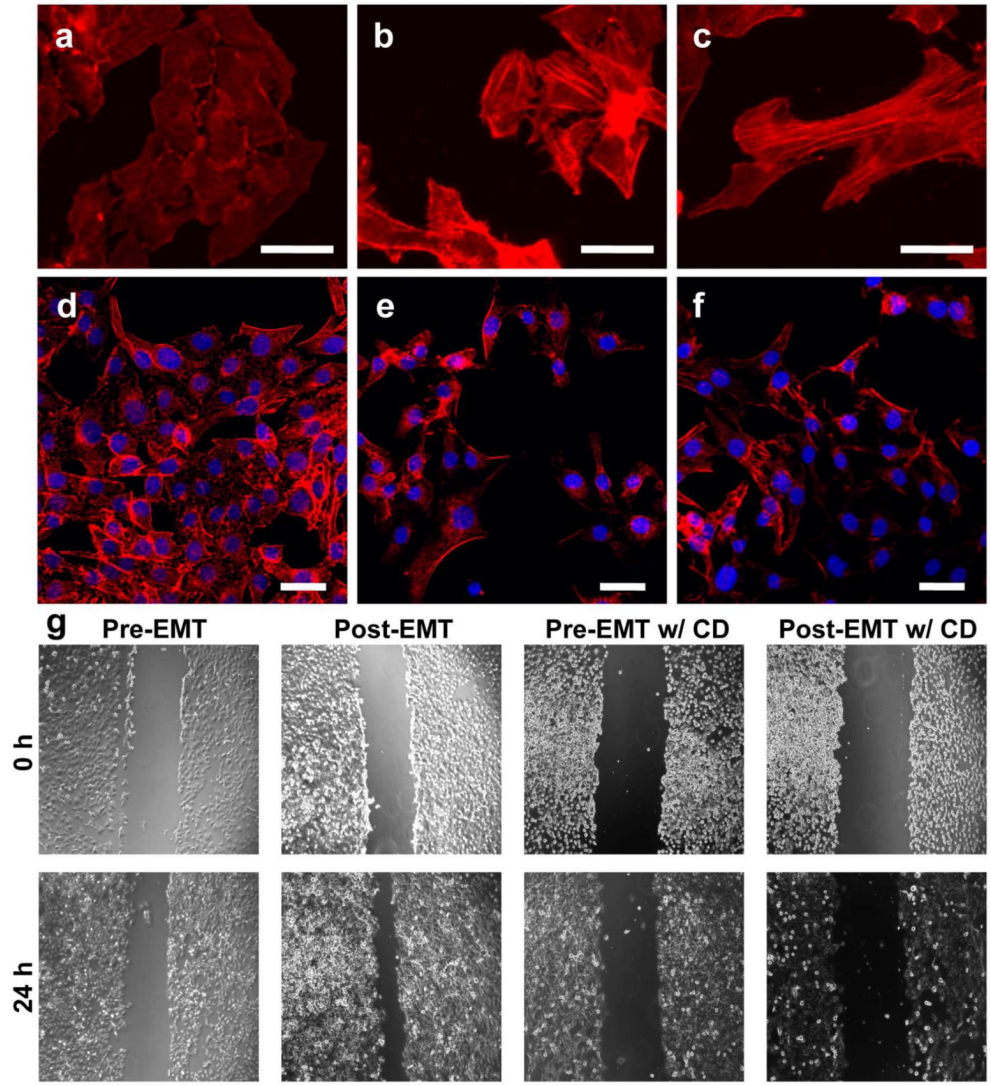

Figure 4.

Morphological changes and migration assay of SKOV-3 cells upon EMT induced by TGF-β. Untreated SKOV-3 cells (a, d) and after treatment with 10 ng/mL (b, e) and 20 ng/mL (c, f) of TGF-β for 24 h (40× magnification for (a-c) and 25× magnification for (d-f), scale bars: 50 μm). The red fluorescence is from the actin cytoskeleton stained with phalloidin-TRITC and the blue fluorescence is from cell nuclei stained by DAPI. TGF-β-treated SKOV-3 cells demonstrate the elongated and dispersed morphology characteristic of the post-EMT cells (b, c, e, and f), compared to pre-EMT SKOV-3 cells that form dense colonies (a, d).[1] Cell aspect ratios were quantified using ImageJ software. At least 200 cells were measured in each treatment group. The average aspect ratios expressed as mean ± standard error were 1.44 ± 0.04 (a, d); 3.38 ± 0.15 in (b, e); and 4.19 ± 0.21 in (c, f. g). Nearly confluent SKOV-3 cells scratched with a pipette tip and wound-healing rates were observed after 24 h with and without 20 ng/mL of TGF-β and 4 μM of CD. Scale bars: 200 μm. The wound areas of treated and control groups were quantified using ImageJ software and expressed as mean ± standard deviation (n=4). The wound area relative to original wound area was 0.79 ± 0.14 in pre-EMT cells; 0.50 ± 0.04 in post-EMT cells; 0.98 ± 0.05 in pre-EMT cells with CD; and 0.91 ± 0.05 in post-EMT cells with both TBF-β and CD.

NIH-PA Author Manuscript
NIH-PA Author Manuscript
NIH-PA Author Manuscript

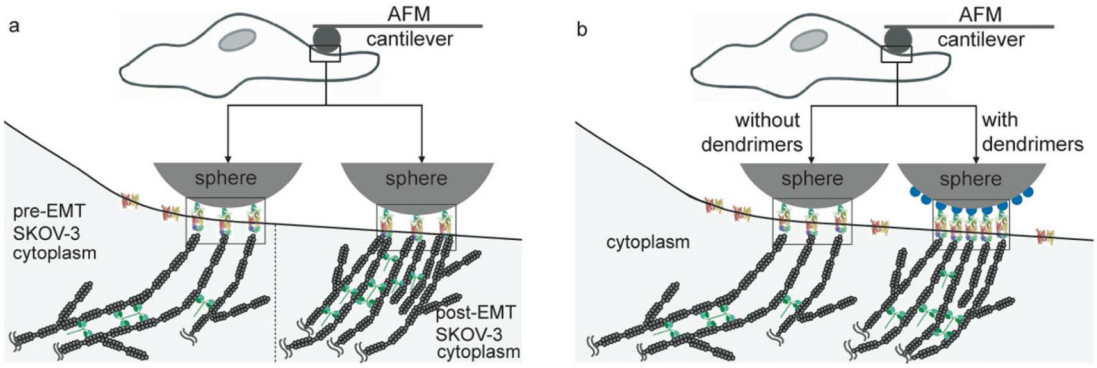

Figure 5.

Schematic of focal adhesion formation and force transmission by FN-integrin α5β1 pairs. The direct contact of fibronectin-conjugated AFM probes on the surface of ovarian cancer cells triggers the formation of focal adhesions, in which FN-integrin pairs are clustered and the actin cytoskeleton is physically associated. This physical connection of the actin cytoskeleton, integrin α5β1, FN, and the probe enabled a direct transmission of actin-mediated force to the probe and the measurement of real-time force dynamics. The actin-myosin II interaction or actin polymerization/depolymerization dynamics generate mechanical forces, which are recorded as real-time deflection (Figure 1 and 2). (**a)** In both pre- and post-EMT SKOV-3 cells, the numbers of the FN-integrin pairs in the focal adhesion are estimated to be the same because the number of FN immobilized on the spherical AFM probe surface confine the number of FN-integrin pairs in the focal adhesion; therefore, the larger magnitude of forces measured on post-EMT cells indicate that larger quantities of the actin cytoskeleton are conjugated to the focal adhesion on the post-EMT cells than those on pre-EMT cells. G7 dendrimers, represented as blue dots on the surface of the sphere shown in (**b**), enhance the molecular conjugation efficiency of FN and the sensitivity of the force measurement: this increase in the conjugation efficiency of FN and the sensitivity of the force measurement is attributed to an increased number of clustered FN-integrin α5β1 pairs in focal adhesions as discussed. Red-yellow complexes represent integrin α5β1 dimers; green objects on the surface of spheres, FN molecules; gray fibers in the cytoplasmic space, actin cytoskeletal filaments; green objects between actin cytoskeletal fibers, myosin II that generates mechanical forces via the interaction with the actin cytoskeleton.